A Journal of the Gesellschaft Deutscher Chemiker

Angewandte Chemie

GDCh

International Edition

www.angewandte.org

Accepted Article

Title: Highly Selective and Catalytic Oxygenations of C-H and C=C Bonds by a Mononuclear Nonheme High-Spin Iron(III)−Alkylperoxo Species

Authors: Tapan Kanti Paine, Ivy Ghosh, Sridhar Banerjee, Satadal Paul, and Teresa Corona

To be cited as: *Angew. Chem. Int. Ed.* 10.1002/anie.201906978
Angew. Chem. 10.1002/ange.201906978

Link to VoR: http://dx.doi.org/10.1002/anie.201906978
http://dx.doi.org/10.1002/ange.201906978

WILEY-VCH

Angewandte Communications

Bioinspired Catalysis

DOI: 10.1002/anie.201((will be filled in by the editorial staff))

Highly Selective and Catalytic Oxygenations of C-H and C=C Bonds by a Mononuclear Nonheme High-Spin Iron(III)–Alkylperoxo Species**

*Ivy Ghosh,[a] Sridhar Banerjee,[a] Satadal Paul,[b] Teresa Corona,[c] and Tapan Kanti Paine [a,]**

Dedicated to Professor Phalguni Chauduri on His 75th Birthday

*The reactivity of a mononuclear high-spin iron(III)-alkylperoxo intermediate [Fe^{III}(t-BuL^{Urea})(OOCm)(OH$_2$)]$^{2+}$(**2**), generated from [Fe^{II}(t-BuL^{Urea})(H$_2$O)(OTf)](OTf) (**1**) (t-BuL^{Urea}= 1,1'-(((pyridin-2-ylmethyl)azanediyl)bis(ethane-2,1-diyl))bis(3-(tert-butyl)urea), OTf = trifluromethanesulfonate) with cumyl hydroperoxide (CmOOH), toward the C-H and C=C bonds of hydrocarbons is reported. Intermediate **2** oxygenates the strong C-H bonds of aliphatic substrates with high chemo- and stereo-selectivity in the presence of 2,6-lutidine. While **2** itself is a sluggish oxidant, 2,6-lutidine assists the heterolytic O-O bond cleavage of the metal-bound alkylperoxo giving rise to a reactive metal-based oxidant. The role of urea groups on the supporting ligand and of the base in directing the selective and catalytic oxygenation of hydrocarbon substrates by **2** are presented.*

Dioxygen-activating heme and nonheme iron enzymes involve iron-oxygen species such as iron(III)-superoxide, iron(III)-peroxide, iron(II/III)-hydro/alkylperoxo and iron(IV/V)-oxo as active oxidants depending upon enzymatic functions.[1-4] The iron-hydro/alkylperoxo (Fe-OOR(H)) species, proposed as key intermediates in several enzymatic reactions,[5, 6] have attracted considerable attention in synthetic biomimetic chemistry. A number of nonheme iron(III)-alkylperoxo intermediates have been prepared and characterized over the last couple of decades.[4, 7-9] The bioinspired studies provided useful information about the electronic and structural features of these intermediates and their use in the generation of high-valent iron-oxo species.[3, 4, 8, 10-14] While the heterolytic O-O bond cleavage of a dioxygen-derived Fe-OOR(H) intermediate forms a high-valent iron-oxo species in enzymatic systems,[2, 6] the O-O/Fe-O bonds of synthetic Fe(III)-OOR(H) are often cleaved homolytically.[14-16] Among other factors, spin states of the metal centre have been reported to play important roles in modulating the strength of Fe–O and O–O bonds, and their cleavage in nonheme Fe(III)-OOR species.[12, 17] In the Fe-O bond homolysis, a high-spin iron(III)-OOR would produce peroxyl radical, which often leads to uncontrolled oxidation of substrates in alkylperoxide-dependent catalytic oxidations by iron complexes.[18] Recent reports indicated that different strategies such as use of protic/Lewis acid, or use of secondary coordination interactions could direct the heterolytic O-O cleavage of iron-OOR (R = H, acyl) species.[19-22] Direct formation of iron(IV)-oxo species from iron(II) precursor complexes and hydrogen peroxide have been reported without generation of iron(III)-hydroperoxo intermediates.[16, 19, 23, 24] A putative iron(II)-OOR(H), generated *in situ* upon one-electron reduction of the iron(III)-intermediate, has been proposed to undergo heterolytic O-O bond cleavage resulting in the formation of the corresponding iron(IV)-oxo species.[11, 25] Applying all these strategies, selectivity in iron-catalyzed oxidations was achieved using hydrogen peroxide or acylperoxides. In some cases, highly reactive metastable iron-oxo oxidants were trapped and characterized. On the contrary, nonheme Fe(III)-OOR species have been reported as sluggish oxidant in oxygenation reactions[13] and tuning their stability[26] and controlling the O-O bond heterolysis is less explored.[21, 27] Therefore, selective and catalytic oxygenation particularly of strong C-H bonds using alkylperoxides remains a challenge in bioinspired catalysis.

In that direction, we have investigated the catalytic activity of an iron(II)-triflate complex, [Fe^{II}(*t*-BuL^{Urea})(H$_2$O)(OTf)](OTf) (**1**) supported by a tetradentate ligand (*t*-BuL^{Urea} = 1,1'-(((pyridin-2-ylmethyl)azanediyl)bis(ethane-2,1-diyl))bis(3-(*tert*-butyl)urea), OTf = trifluromethanesulfonate) (Scheme 1) containing two urea groups toward different substrates using cumyl hydroperoxide. As a result of our investigation, we report herein the reactivity of a high-spin

[*] (a) Ms. I. Ghosh, Mr. S. Banerjee, Prof. T. K. Paine
School of Chemical Sciences Indian Association for the Cultivation of Science, 2A & 2B Raja S. C. Mullick Road, Jadavpur, Kolkata-700032, India. Fax: (+)91-33-2473-2805
E-mail: ictkp@iacs.res.in
(b) Dr. S. Paul, Darjeeling Polytechnic, Kurseong, Darjeeling 734203, India
(c) Dr. T. Corona, Humboldt-Universität zu Berlin, Department of Chemistry, Brook-Taylor-Strasse 2, 12489 Berlin, Germany

[**] TKP acknowledges SERB, India for the financial support (Project: EMR/2014/000972). SB thanks CSIR, India, for a research fellowship and TC thanks the Alexander von Humboldt Foundation for a postdoctoral grant. The authors acknowledge Reza G. Shirazi of Max-Planck-Institut für Kohlenforschung for the help with computational studies.

Supporting information for this article is available on the WWW under http://dx.doi.org/10.1002/anie.201xxxxxx.

10.1002/anie.201906978

iron(III)-cumylperoxo, $[Fe^{III}(t\text{-}BuL^{Urea})(OOCm)(OH_2)]^{2+}$ (**2**) in chemo- and stereoselective oxygenation of aliphatic C-H and olefin C=C bonds under stoichiometric and catalytic conditions in the presence and absence of 2,6-lutidine. The stability of the iron(III)-cumyl peroxo intermediate on the urea-group bearing ligand and its reactivity in the presence of a general base in comparison to that of a related iron complex, $[Fe^{II}(Me_4\text{-benpa})(OTf)_2]$ (**3**)[28] (Me_4-benpa = N^1-(2-(dimethylamino)ethyl)-N^2,N^2-dimethyl-N^1-(pyridin-2-ylmethyl)ethane-1,2-diamine), with the supporting ligand devoid of urea groups are presented in this work.

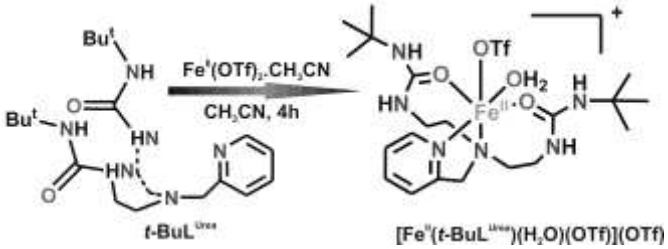

Scheme 1 Synthesis of $[Fe^{II}(t\text{-}BuL^{Urea})(H_2O)(OTf)]^+$ (**1**).

The tetradentate t-BuL^{Urea} ligand was prepared following the procedure reported in literature.[29] The iron(II) complex $[Fe^{II}(t\text{-}BuL^{Urea})(H_2O)(OTf)](OTf)$ (**1**) was isolated as a light brown solid from the reaction of equimolar amounts of $Fe(OTf)_2{\cdot}2MeCN$ and t-BuL^{Urea} in acetonitrile (Scheme 1 and Experimental Section, Supporting Information, SI). The ESI-mass spectrum (positive ion mode in acetonitrile) of compound **1** displays an ion peak at m/z = 597.2 with the isotope distribution pattern calculated for $[Fe(t\text{-}BuL^{Urea})(OTf)]^+$ (Figure S1, SI). Paramagnetically shifted proton resonances in the region between -10 ppm and 70 ppm (Figure S2, SI), typical of high-spin iron centre, are observed in ^1H NMR spectrum of **1** in CD_3CN at 298 K. The ^{19}F NMR spectrum of the complex in CD_3CN, displays a sharp resonance at -81 ppm, whereas a relatively broad signal appears at -47 ppm in $CDCl_3$ (Figures S3 and S4, SI). The NMR features clearly suggest that acetonitrile replaces the coordinated triflate and a slow exchange takes place between triflate and acetonitrile.[28] In contrast, a fast exchange between the coordinated and the free triflate takes place in the non-coordinating solvent, $CHCl_3$. Although the spectral and analytical data unambiguously support the composition of complex **1**, attempts to isolate X-ray quality single crystals for structural characterization failed. Therefore, the structure of a ternary iron(II) complex $[Fe(t\text{-}BuL^{Urea})(DBHD)](OTf)_2$ (**4**) (DBHD = N^1,N^2-di-*tert*-butylhydrazine-1,2-dicarboxamide)[30] was relied (Experimental section and Table S1, SI) to gain information about the binding mode of the ligand, t-BuL^{Urea}. The structure of the dication **4** reveals that the t-BuL^{Urea} ligand binds to the iron centre through one pyridine nitrogen (Fe1-N1 at 2.166 Å), one amine nitrogen (at 2.313 Å) and two oxygen donors of the urea groups (at an average Fe-O_{urea} distance of 2.05 Å) (Figure S5 and Table S2, SI). The co-ligand (DBHD) binds in a bidentate fashion through one hydrazine nitrogen and one amide oxygen resulting in a distorted octahedral coordination geometry at the metal centre. DFT calculations predict that the metal-ligand bond distances in six-coordinate complex $[Fe^{II}(t\text{-}BuL^{Urea})(H_2O)(OTf)](OTf)$ **(1)** with the N_2O_2-bound ligand closely match to those of **4** further supporting the high-spin nature of **1** (Table S3 and S4, and Figure S6, SI). The higher stability of N_2O_2 coordinated complex can be attributed to the shorter M-O (equatorial) bonds compared to the metal-N(equatorial) distances in the N_4 coordinated form. It is to mention here that the doubly deprotonated form of the t-BuL^{Urea} ligand has been reported to coordinate in N_4 binding mode stabilizing the low-spin (S = 0) iron(II) complex.[29] The six-coordinate high-spin species was further confirmed by the zero-field ^{57}Fe Mössbauer spectrum of the **1** in acetonitrile at 17 K displaying the isomer shift (δ) and quadrupole splitting (ΔE_Q) values of 1.28 mms^{-1} and 3.40 mms^{-1}, respectively (Figure S7, SI). Since the coordinated triflate in **1** undergoes slow exchange with acetonitrile, ΔE_Q for the six-coordinate complex $[Fe^{II}(t\text{-}BuL^{Urea})(CH_3CN)(H_2O)](OTf)_2$ (**1a**) with N_2O_2-bound ligand was also calculated. The calculated value (3.34 mms^{-1}) of **1a** closely matches with the experimental value (Table S5, SI) and also with the calculated value (3.39 mms^{-1}) for **1**.

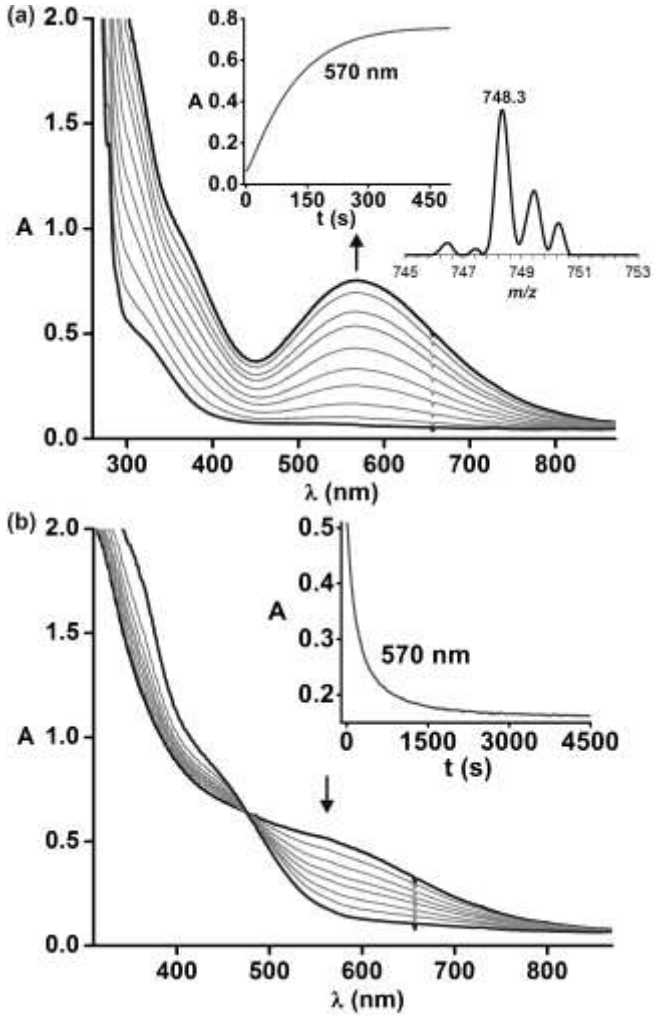

Figure 1 (a) Formation of **2** upon treatment of **1** (0.5 mM) with CmOOH in acetonitrile at –20°C. Inset: time trace for the band at 570 nm and the isotope distribution pattern of the ion peak at m/z 748.3. (b) Decay of **2** at 10°C in the presence of 2,6-lutidine (1 equiv) along with the time trace (inset).

Complex **1** upon treatment with cumyl hydroperoxide (CmOOH) (10 equiv) in acetonitrile at -20°C produces a deep blue species showing an absorption band at 570 nm (Figure 1a). The spectral feature, originates from the peroxide to iron(III) charge-transfer transition, bears resemblance to other reported iron(III)-alkylperoxide species.[21] The ESI-mass spectrum of the intermediate species displays ion peaks at m/z 748.3 and 614.2 with the isotope distribution patterns attributable to $[^{56}Fe^{III}(t\text{-}BuL^{Urea})(OOCm)(OTf)]^+$ and $[^{56}Fe^{III}(t\text{-}BuL^{Urea})(OH)(OTf)]^+$ respectively (Figure 1a, Inset and Figure S8, SI). The latter peak likely arises from the decomposition of the intermediate species

10.1002/anie.201906978

under the mass sepctroscopic conditions. The composition of the ion peak was further supported by the mass spectrum of the intermediate generated from the ^{57}Fe-enriched sample of **1** (Figure S9, SI). The X-band EPR spectrum of the intermediate on a frozen sample at 4 K exhibits a strong signal at g = 4.25 along with a less intense signals at g = 9.20, 4.80 and 3.87 (Figure S10, SI). The broadness of the resonance signals suggests the presence of two S = 5/2 iron(III) species with different rhombicities (E/D = 0.33 and 0.22, respectively). The ^{57}Fe Mössbauer spectrum of the frozen sample of the intermediate in acetonitrile collected in zero field at 17 K displays three quadrupole doublets with two Fe(III) species of 1:1 ratio along with the precursor Fe(II) complex (33%) (Figure 2). Both the iron(III) species, generated upon treatment of **1** with CmOOH, coexist and represent 67% of the total intermediate. Considering that amount of intermediate, the extinction coefficient of the intermediate is estimated to be 2200 $M^{-1}cm^{-1}$, a value close to the reported high-spin iron(III)-alkylperoxide intermediates. To gain insights into the two probable co-existing iron(III) specie, as indicated by EPR and Mössbauer data, different variants (five-coordinate vs six-coordinate, and $H_2O/MeCN/OH^-$ as the sixth ligand for six-coordinate species) of the iron(III)-OOCm species and also the iron(III)-OH decomposition product (as observed in the mass spectrum) were investigated by DFT optimization (Table S5, SI). Among those, the six-coordinate iron(III)-OOCm species with an equatorial water ligand for both N_2O_2 and N_4-coodinated ligand (Tables S6 and S7, and Figure S11, SI) produce spectral features similar to those observed experimentally (Figure S12, SI). While both the six-coordinate iron(III)-OOCm species are energetically close, the one with N_2O_2-coordinated ligand should be more stable due to stronger bonding through equatorial oxygen donors of urea groups compared to that in N_4-coordinated ligand. However, the energy difference between the two species diminishes due to the presence of hydrogen bonding interactions in the iron(III)-OOCm species with N_4-coordinated ligand. Additionally, the calculated quadrupole splitting ΔE_Q value of 1.53 mms^{-1} of the six-coordinate iron(III)-OOCm species with N_2O_2-bound ligand is quite close to the experimental one (1.77 mms^{-1}) (Table S5, SI). Although no other form of the iron(III)-OOCm species could theoretically produce the other ΔE_Q value (0.69 mms^{-1}), the experimental results support the co-existence of a structurally and energetically similar to the $[Fe^{III}(t\text{-}BuL^{Urea})(OOCm)(H_2O)]^{2+}$ (**2**), which may include its linkage isomer and/or deprotonated state.

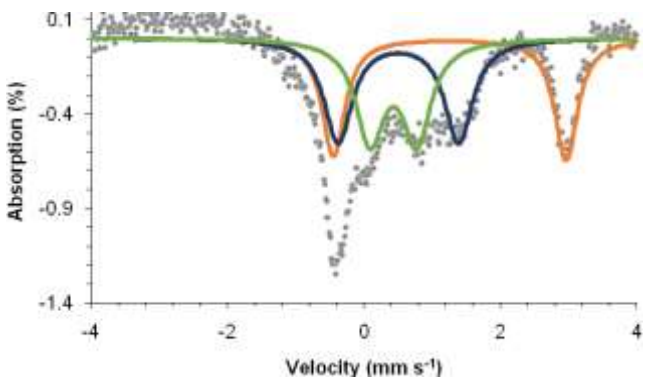

Figure 2 The zero-field Mössbauer spectrum of **2** (^{57}Fe enriched in acetonitrile) recorded at 17 K. The solid lines represent fits of the experimental spectrum (dots)with Lorentzian quadrupole doublet, the major component (34%, deep blue line, ΔE_Q = 1.77 mm s^{-1} and δ = 0.51 mm s^{-1}) and (33%, green line, ΔE_Q = 0.69 mm s^{-1} and δ = 0.43 mm s^{-1}) corresponds to intermediate species (**2**), the minor component (33%, orange line, ΔE_Q = 3.41 mm s^{-1} and δ = 1.26 mm s^{-1}) corresponds to unreacted iron(II) complex.

The intermediate **2** is quite stable at -20°C, but decays at 10°C following a pseudo-first order kinetics with the $t_{1/2}$ of 23 min (Figure S13, SI). The fact that neither the $[Fe^{II}(Me_4\text{-benpa})(OTf)_2]$ (**3**) complex nor the iron(II) complex of the deprotonated t-BuL^{Urea} form any intermediate species from CmOOH under similar experimental conditions. However, the iron(II) complex $[Fe^{II}(t\text{-}BuL^{Py2,Urea})(OTf)_2]$ **(5)** (t-$BuL^{Py2,Urea}$ = 1-(2-(bis(pyridin-3-ylmethyl)amino)ethyl)-3-*tert*-butylurea) of a monourea analogue of t-BuL^{Urea} ligand (Experimental Section, SI) forms a similar iron(III)-CmOOH intermediate (Figure S14, SI) but is less stable ($t_{1/2}$ = 2 min at 10°C) compared to **2** highlighting the role played by the supporting ligand in the formation and stabilization of the intermediate.[9]

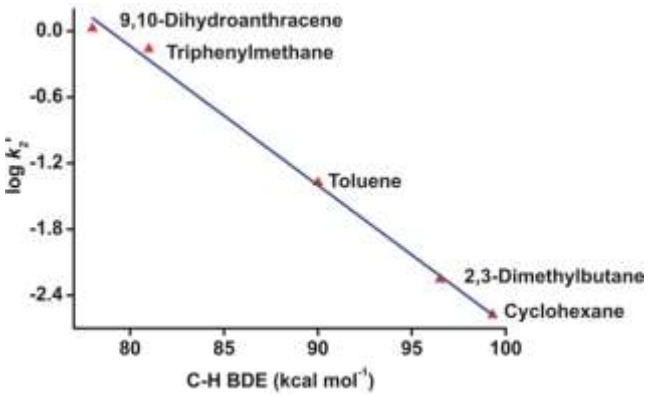

Figure 3 Plot of log k_2' versus C-H bond dissociation energies of different substrates in the reaction with **2**. k_2' is obtained by dividing the second-order rate constant by the number of abstractable C-H bonds in a substrate.

Since CmOOH is known as a useful mechanistic probe to differentiate between homolytic and heterolytic O-O bond cleavage pathway,[21, 31] the product analysis after decay of **2** reveals the formation of a mixture of cumyl alcohol and acetophenone in a 5:1 ratio. Thus, the O-O bond cleavage operates in both homolytic and heterolytic fashion. Interestingly, the decay of **2** follows a clear isosbestic point with the $t_{1/2}$ value of 3 min upon addition of one equiv of 2,6-lutidine (Figure 1b). The increased decay rate and the formation of cumyl alcohol as the exclusive product suggest the O-O bond heterolysis of **2** mediated by 2,6-lutidine. The decay kinetics of **2** in the presence of aliphatic substrates (20-400 equiv) follow pseudo-first order and the observed rate constants depend linearly on the substrate concentration (Figures S15 and S16, SI). The second order rate constant (k_2) at 283 K thus obtained for a series of substrates having C-H bond dissociation energies (BDE's) ranging 78-99.3 kcal/mol[32] were used to understand the hydrogen atom transfer (HAT) reactivity. The corrected k_2' values based on the number of abstractable C-H bonds exhibit good linear correlation between log k_2' and C-H bond dissociation energy (C-H BDE) of substrates (Figure 3). This linear correlation suggests that the substrate oxidation by the oxidant generated in the system takes place via the rate-determining HAT pathway. Similar correlation has been established for HAT reaction by high-valent iron-oxo complexes.[33]

The second order rate constants for separate reactions of **2** with toluene and toluene-d_8 in the presence of 2,6-lutidine at 283 K afford a primary kinetic isotope effect (KIE) value of 13.3 (Figure S16, SI). The KIE value in cyclohexane oxidation is found to be 7.2, further supporting the C-H bond abstraction by a metal-based oxidant being

10.1002/anie.201906978

the rate-limiting step.[34] The KIE values obtained in toluene and cyclohexane oxidation in the absence of 2,6-lutidine are 5.7 and 1.6, respectively (Figure S16, SI). These results are in line with the observed heterolytic O-O cleavage with 2,6-lutidine, whereas both homolytic and heterolytic pathways are operational without 2,6-lutidine. Furthermore, the solvent KIE value of 1.4, determined by the ratio of decay rate of **2** in the presence of 2,6-lutidine in CH_3CN and CD_3CN, support the involvement of 2,6-lutidine in involving a proton to facilitate the heterolytic O-O bond cleavage and in the formation of a high-valent metal-based oxidant. While no such intermediate species was detected in the decay process, the *in situ* generated species was intercepted using aliphatic substrates (Scheme S1, SI). The reaction of complex **1** with cyclohexane with CmOOH (10 equiv) and 2,6-lutidine (1 equiv) reveals the formation of cyclohexanol (TON 1.1) and cyclohexanone (2%) with an alcohol to ketone ratio (A/K) of 55 (Figure S17, SI). Increasing the equivalent of base and the reaction time beyond 1 h does not change the product profile. In the absence of 2,6-lutidine, however, low selectivity with the A/K ratio of 5 is observed for cyclohexane oxidation. The oxidant is found to oxidize adamantane with a C3/C2 normalized selectivity of 16.5 using 2,6-lutidine, which is reduced to 5.9 without the base (Figure S18, SI). Methylcyclohexane is oxygenated to form the 3° alcohol selectively. A lighter alkane, 3-methyl pentane affords the corresponding alcohol in 27% yield. In the absence of lutidine, radical species generated in the decay of **2** via homolytic O-O cleavage pathway gives rise to non-selective oxidation of substrates (Scheme S1, SI).

Considering the selective oxygenation of tertiary C-H bonds by the active oxidant, the stereoselectivity in the hydroxylation was tested with a number of substrates (Scheme 2). *cis*-1,2-Dimethylcyclohexane affords the corresponding tertiary alcohol product in 96% yield with 96% retention of configuration (RC) (Figure S19, SI). Similarly, *trans*-1,2-dimethylcyclohexane displays 92% RC selectivity (Figure S19, SI). In the absence of 2,6-lutidine, only 12% of tertiary alcohol was obtained with less selectivity (71% RC) for *cis*-1,2-dimethylcyclohexane. In the cases of *cis*-decalin and *trans*-decalin, the yields of tertiary alcohol products increase in the presence of 2,6-lutidine exhibiting RC selectivity of 94% and 88%, respectively (Scheme 2 and Figure S20, SI). Thus, addition of 2,6-lutidine not only increases the reactivity of the oxidant but also improves the RC selectivity. The observed RC selectivity is consistent with that reported in H_2O_2 and peracetic acid-dependent oxidation by nonheme iron(II) complexes using protic acids.[22]

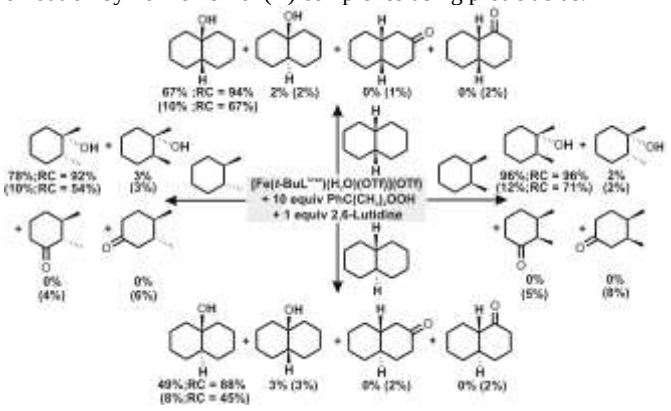

Scheme 2 Stereoselective oxygenation of aliphatic C-H bonds of different substrates by complex **1** with CmOOH (10 equiv). The values in the brackets indicate the yields in the absence of 2,6-lutidine. %RC = 100 X (*cis*-*trans*)/(*cis*+*trans*) in case of *cis*-isomer or 100 X (*trans*-*cis*)/(*cis*+*trans*) in case of *trans*-isomer.

The active oxidant generated from **2** is also capable of performing oxygen atom transfer reaction (OAT) to alkenes. While, the alkenes such as cyclohexene, styrene, cyclooctene and 1-octene afford non-selective product without 2,6-lutidine, the corresponding epoxides are obtained as major products with 2,6-lutidine (Scheme S2, SI). Notably, *cis*-2-heptene forms the corresponding *cis*-epoxide (TON 1.1) as the sole product in the presence of base (Figure S21, SI). The oxidant, therefore, performs stereoselective OAT reaction to alkenes. Of note, complex $[Fe^{II}(Me_4\text{-benpa})(OTf)_2]$ (**3**) displays non-selective oxidation of the aforementioned substrates under similar experimental conditions (Scheme S3, SI). The oxidations with **3** primarily proceed via radical pathway as evident from the inhibition of product formation in the presence of radical scavengers. However, the radical scavenger does not change the yield of substrate-derived products in the oxidation with **2** (Table S8, SI). Furthermore, the iron(II) complex of the double deprotonated form of the *t*-BuL^{Urea} ligand does not show oxygenation of the substrates with CmOOH. It is important to mention that the high-spin iron(III)-OOCm species, $Fe^{III}(6\text{-}Me_3\text{-TPA})(OOCm)]^{2+}$ in combination with 2.6-lutidine does not perform selective oxygenation under similar experimental conditions. All these results implicate the role played by the urea groups and lutidine in controlling the heterolytic O-O bond cleavage and subsequent reactivity by metal-based oxidant from **2**.

Considering the high yield of oxygenated products in the reaction of **1** with substrates and 2,6-lutidine, the catalytic potential of the complex was investigated (Figures S22 and S23, SI). Increasing the amount of CmOOH from 10 to 50 equiv increases the TON of cyclohexanol from 1.1 to 16 (Figure S24, SI). In addition, the TON for cyclohexanol increases to 21 by increasing the amount of cyclohexane from 100 to 500 equiv (Figure S25, SI). The yield of cyclohexanol further increases to a TON of 37 upon adding 250 equiv of CmOOH and 1 equiv of 2,6-lutidine in every hour (Figure S26, SI). However, with excess CmOOH, overoxidation of cyclohexanol to cyclohexanone takes place. These results under the optimized conditions reveal that the complex can perform selective and catalytic HAT and OAT reactions with moderate TONs (Table 1).

Table 1 Catalytic oxygenation of substrates by complex **1** using CmOOH as the oxidant.

Substrate (500 equiv)	**Product**	**TON[a]**
1-Octene	2-Hexyloxirane	42 ± 0.7
Cyclooctene	9-Oxabicyclo[6.1.0]nonane	26 ± 0.4
Styrene	2-Phenyloxirane Benzaldehyde	9 ± 0.1 5 ± 0.2
Cyclohexene	Cyclohexene oxide 2-Cyclohexen-1-ol	25 ± 0.8 4.5 ± 0.2
cis-2-Heptene	*cis*-2-Butyl-3-methyl oxirane	7 ± 0.4
Toluene	Benzyl alcohol Benzaldehyde	9 ± 0.4 0.5 ± 0.02
Cyclohexane	Cyclohexanol Cyclohexanone	21 ± 0.5 0.3 ± 0.01
Methyl cyclohexane	1-Methyl cyclohexanol 2-Methyl cyclohexanol	21 ± 0.6 0.2 ± 0.01
3-Methyl pentane	3-Methyl pentanol	0.8 ± 0.02
cis-1,2-Dimethyl cyclohexane	*cis*-1,2-Dimethylcyclohexanol	3 ± 0.1
trans-1,2-Dimethyl cyclohexane	*trans*-1,2-Dimethylcyclohexanol	2.5 ± 0.1
cis-Decalin	*cis*-4-Decalol	13 ± 0.3
trans-Decalin	*trans*-4-Decalol	9 ± 0.2

*Experimental conditions: 0.01 mmol complex **1**, 50 equiv of $PhC(CH_3)_2OOH$ and 1 equiv of 2,6-lutidine in acetonitrile at 253 K. Reaction time: 1 h at 283 K after generation of intermediate. [a]Turnover number (TON) = mol of product/mol of catalyst.*

The selective oxidations of substrates are performed by a metal-based oxidant from $[Fe^{III}(t\text{-}BuL^{Urea})(OOCm)(OH_2)]^{2+}$ mediated by a general base. The NH groups of urea and nitrogen of 2,6-lutidine are known to form H-bonds.[35] The H-bonded pyridine base subsequently takes up a proton from the iron-coordinated urea group. The conjugate acid thus formed facilitates the heterolytic O-O bond cleavage through hydrogen bonding interaction[24] with the distal oxygen of the peroxide unit (Scheme S4, SI) resulting in the generation of a putative iron(V)-oxo oxidant, which performs substrate oxidation. In the absence of the base, the minor pathway involving spontaneous deprotonation of the urea group likely forms the active oxidant displaying oxidations but with low selectivity. However, further mechanistic studies are required to gain information about the active oxidant involved in the reaction pathway.

In summary, the isolation and characterization of an iron(II) complex of a tetradentate ligand containing urea groups is reported. The ligand stabilizes the corresponding high-spin iron(III)-cumylperoxo species, which decays upon addition of 2,6-lutidine undergoes heterolytic O-O bond cleavage resulting in the generation of a putative high-valent metal-oxo intermediate. The metal-based oxidant is able to oxygenate the strong C-H bonds of alkanes with high chemo- and stereo-selectivity. The high A/K ratio (55) and KIE value (7.2) in cyclohexane oxidation strongly support the C-H bond abstraction by the active oxidant being the rate-limiting step. Moreover, the complex displays catalytic HAT and OAT reactions with high selectivity. The results presented here shows the importance of urea group on ligand backbone and of a general base in directing the course of reactivity of otherwise sluggish iron(III)-alkylperoxo oxidant. Further experimental and computational studies in elucidating the mechanism of the reaction are presently being carried out in our laboratory.

Receive: ((will be filled in by the editorial staff))
Published online on ((will be filled in by the editorial staff))

Keywords: Nonheme • Iron • Alkylperoxide • Catalytic oxidation • Stereoretention

[1] (a) S. Kal, L. Que, Jr., *J. Biol. Inorg. Chem.* **2017**, *22*, 339; (b) C. J. Knoot, V. M. Purpero, J. D. Lipscomb, *Proc. Natl. Acad. Sci. U. S. A.* **2015**, *112*, 388; (c) J. Rittle, M. T. Green, *Science* **2010**, *330*, 933; (d) P. C. A. Bruijnincx, G. van Koten, R. J. M. K. Gebbink, *Chem. Soc. Rev.* **2008**, *37*, 2716; (e) C. Krebs, D. G. Fujimori, C. T. Walsh, J. M. Bollinger, Jr., *Acc. Chem. Res.* **2007**, *40*, 484; (f) P. R. Ortiz de Montellano, J. J. De Voss, Kluwer Academic/Plenum Publishers, New York, **2005**, pp. 183; (g) I. G. Denisov, T. M. Makris, S. G. Sligar, I. Schlichting, *Chem. Rev.* **2005**, *105*, 2253.

[2] S. C. Peck, W. A. van der Donk, *JBIC, J. Biol. Inorg. Chem.* **2017**, *22*, 381.

[3] W. Nam, *Acc. Chem. Res.* **2007**, *40*, 522.

[4] M. Costas, M. P. Mehn, M. P. Jensen, L. Que, Jr., *Chem. Rev.* **2004**, *104*, 939.

[5] (a) J. Cho, R. Sarangi, W. Nam, *Acc. Chem. Res.* **2012**, *45*, 1321; (b) E. G. Kovaleva, J. D. Lipscomb, *Nat. Chem. Biol.* **2008**, *4*, 186; (c) E. G. Kovaleva, J. D. Lipscomb, *Science* **2007**, *316*, 453

[6] P. F. Fitzpatrick, *Biochemistry* **2003**, *42*, 14083.

[7] (a) S. Sahu, D. P. Goldberg, *J. Am. Chem. Soc.* **2016**, *138*, 11410; (b) Y. Zang, J. Kim, Y. Dong, E. C. Wilkinson, E. H. Appelman, L. Que, Jr., *J. Am. Chem. Soc.* **1997**, *119*, 4197; (c) S. Ménage, E. C. Wilkinson, L. Que, Jr., M. Fontecave, *Angew. Chem. Int. Ed.* **1995**, *34*, 203; (d) J. Kim, E. Larka, E. C. Wilkinson, L. Que, Jr., *Angew. Chem. Int. Ed.* **1995**, *34*, 2048; (e) A. Company, J. Lloret-Fillol, M. Costas, in *Comprehensive Inorganic Chemistry II (Second Edition)* (Eds.: J. Reedijk, K. Poeppelmeier), Elsevier, Amsterdam, **2013**, pp. 487.

[8] (a) J. Cho, S. Jeon, S. A. Wilson, L. V. Liu, E. A. Kang, J. J. Braymer, M. H. Lim, B. Hedman, K. O. Hodgson, J. S. Valentine, E. I. Solomon, W. Nam, *Nature* **2011**, *478*, 502; (b) D. Krishnamurthy, G. D. Kasper, F. Namuswe, W. D. Kerber, A. A. Narducci Sarjeant, P. Moënne-Loccoz, D. P. Goldberg, *J. Am. Chem. Soc.* **2006**, *128*, 14222; (c) S. Gosiewska, H. P. Permentier, A. P. Bruins, G. van Koten, R. J. M. K. Gebbink, *Dalton Trans.* **2007**, 3365.

[9] L. R. Widger, Y. Jiang, A. C. McQuilken, T. Yang, M. A. Siegler, H. Matsumura, P. Moënne-Loccoz, D. Kumar, S. P. de Visser, D. P. Goldberg, *Dalton Trans.* **2014**, *43*, 7522.

[10] (a) K. Ray, F. F. Pfaff, B. Wang, W. Nam, *J. Am. Chem. Soc.* **2014**, *136*, 13942; (b) A. R. McDonald, L. Que, Jr., *Coord. Chem. Rev.* **2013**, *257*, 414; (c) E. Nam, P. E. Alokolaro, R. D. Swartz, M. C. Gleaves, J. Pikul, J. A. Kovacs, *Inorg. Chem.* **2011**, *50*, 1592; (d) L. Que, Jr., *Acc. Chem. Res.* **2007**, *40*, 493; (e) M. P. Jensen, A. M. i. Payeras, A. T. Fiedler, M. Costas, J. Kaizer, A. Stubna, E. Münck, L. Que, Jr. *Inorg. Chem.* **2007**, *46*, 2398; (f) J. Bautz, P. Comba, L. Que, Jr. *Inorg. Chem.* **2006**, *45*, 7077; (g) T. Kitagawa, A. Dey, P. Lugo-Mas, J. B. Benedict, W. Kaminsky, E. Solomon, J. A. Kovacs, *J. Am. Chem. Soc.* **2006**, *128*, 14448; (h) M. R. Bukowski, H. L. Halfen, T. A. van den Berg, J. A. Halfen, L. Que Jr, *Angew. Chem. Int. Ed.* **2005**, *44*, 584; (i) N. Lehnert, K. Fujisawa, E. I. Solomon, *Inorg. Chem.* **2003**, *42*, 469; (j) K. Hashimoto, S. Nagatomo, S. Fujiinami, H. Furutachi, S. Ogo, M. Suzuki, A. Uehara, Y. Maeda, Y. Watanabe, T. Kitagawa, *Angew. Chem. Int. Ed.* **2002**, *41*, 1202; (k) J.-J. Girerd, F. Banse, A. J. Simaan, *Struct. Bonding (Berlin)* **2000**, *97*, 145.

[11] S. Bang, S. Park, Y.-M. Lee, S. Hong, K.-B. Cho, W. Nam, *Angew. Chem. Int. Ed.* **2014**, *53*, 7843.

[12] F. Namuswe, T. Hayashi, Y. Jiang, G. D. Kasper, A. A. N. Sarjeant, P. Moënne-Loccoz, D. P. Goldberg, *J. Am. Chemi. Soc.* **2010**, *132*, 157.

[13] M. S. Seo, T. Kamachi, T. Kouno, K. Murata, M. J. Park, K. Yoshizawa, W. Nam, *Angew. Chem., Int. Ed.* **2007**, *46*, 2291.

[14] J. Kaizer, M. Costas, L. Que, Jr., *Angew. Chem. Int. Ed.* **2003**, *42*, 3671.

[15] (a) J. G. McAlpin, T. A. Stich, C. A. Ohlin, Y. Surendranath, D. G. Nocera, W. H. Casey, R. D. Britt, *J. Am. Chem. Soc.* **2011**, *133*, 15444; (b) N. Lehnert, R. Y. N. Ho, L. Que, Jr., E. I. Solomon, *J. Am. Chem. Soc.* **2001**, *123*, 8271.

[16] F. Li, J. England, L. Que, Jr., *J. Am. Chem. Soc.* **2010**, *132*, 2134.

[17] (a) A. Franke, C. Fertinger, R. van Eldik, *Chem. Eur. J.* **2012**, *18*, 6935; (b) F. Namuswe, G. D. Kasper, A. A. N. Sarjeant, T. Hayashi, C. M. Krest, M. T. Green, P. Moënne-Loccoz, D. P. Goldberg, *J. Am. Chem. Soc.* **2008**, *130*, 14189; (c) N. Lehnert, R. Y. N. Ho, L. Que, Jr., E. I. Solomon, *J. Am. Chem. Soc.* **2001**, *123*, 12802; (d) X. Shan, J.-U. Rohde, K. D. Koehntop, Y. Zhou, M. R. Bukowski, M. Costas, K. Fujisawa, L. Que, Jr., *Inorg. Chem.* **2007**, *46*, 8410.

[18] G. Olivo, O. Cussó, M. Borrell, M. Costas, *JBIC J. Biol. Inorg. Chemi.* **2017**, *22*, 425.

[19] K. Cheaib, M. Q. E. Mubarak, K. Sénéchal-David, C. Herrero, R. Guillot, M. Clémancey, J.-M. Latour, S. P. de Visser, J.-P. Mahy, F. Banse, F. Avenier, *Angew. Chem. Int. Ed* **2019**, *58*, 854.

[20] (a) S. Kal, A. Draksharapu, L. Que, Jr., *J. Am. Chem. Soc.* **2018**, *140*, 5798; (b) S. Kal, L. Que, Jr., *Angew. Chem. Int. Ed* **2019**, *doi: 10.1002/anie.201903465*.

[21] Y. Hitomi, K. Arakawa, T. Funabiki, M. Kodera, *Angew. Chem. Int. Ed* **2012**, *51*, 3448.

[22] (a) M. S. Chen, M. C. White, *Science* **2007**, *318*, 783; (b) J. Serrano-Plana, F. Acuña-Parés, V. Dantignana, W. N. Oloo, E. Castillo, A. Draksharapu, C. J. Whiteoak, V. Martin-Diaconescu, M. G. Basallote, J. M. Luis, L. Que, Jr., M. Costas, A. Company, *Chem. Eur. J.* **2018**, *24*, 5331.

[23] J. Bautz, M. R. Bukowski, M. Kerscher, A. Stubna, P. Comba, A. Lienke, E. Münck, L. Que, Jr. , *Angew. Chem. Int. Ed.* **2006**, *45*, 5681.

[24] H. Hirao, F. Li, L. Que, Jr., K. Morokuma, *Inorg. Chem.* **2011**, *50*, 6637.

[25] H. Jeon, S. Hong, *Chem. Lett.* **2019**, *48*, 80.

[26] A. Wada, S. Ogo, Y. Watanabe, M. Mukai, T. Kitagawa, K. Jitsukawa, H. Masuda, H. Einaga, *Inorg. Chem.* **1999**, *38*, 3592.

10.1002/anie.201906978

[27] T. L. Foster, J. P. Caradonna, *J. Am. Chem. Soc.* **2003**, *125*, 3678.
[28] G. J. P. Britovsek, J. England, A. J. P. White, *Inorg. Chem.* **2005**, *44*, 8125.
[29] M. K. Zart, T. N. Sorrell, D. Powell, A. S. Borovik, *Dalton Trans.* **2003**, 1986.
[30] I. Ghosh, T. K. Paine, unpublished data.
[31] (a) S. Hong, Y.-M. Lee, K.-B. Cho, M. S. Seo, D. Song, J. Yoon, R. Garcia-Serres, M. Clémancey, T. Ogura, W. Shin, J.-M. Latour, W. Nam, *Chem. Sci.* **2014**, *5*, 156; (b) M. K. Coggins, V. Martin-Diaconescu, S. DeBeer, J. A. Kovacs, *J. Am. Chem. Soc.* **2013**, *135*, 4260.
[32] Y.-R. Luo, Editor, *Comprehensive Handbook of Chemical Bond Energies*, CRC Press, **2007**.
[33] (a) C. V. Sastri, J. Lee, K. Oh, Y. J. Lee, J. Lee, T. A. Jackson, K. Ray, H. Hirao, W. Shin, J. A. Halfen, J. Kim, L. Que, Jr., S. Shaik, W. Nam, *Proc. Natl. Acad. Sci. U. S. A.* **2007**, *104*, 19181; (b) J. Kaizer, E. J. Klinker, N. Y. Oh, J.-U. Rohde, W. J. Song, A. Stubna, J. Kim, W. Nam, E. Münck, L. Que, Jr., *J. Am. Chem. Soc.* **2004**, *126*, 472.
[34] E. J. Klinker, S. Shaik, H. Hirao, L. Que, Jr., *Angew. Chem. Int. Ed.* **2009**, *48*, 1291.
[35] C. Taouss, P. G. Jones, *CrystEngComm* **2014**, *16*, 5695.

10.1002/anie.201906978

Angewandte Communications

Entry for the Table of Contents

Bioinspired Catalysis

Ivy Ghosh, Sridhar Banerjee, Satadal Paul, Teresa Corona, and Tapan Kanti Paine*

_____ Page – Page

Highly Selective and Catalytic Oxygenations of C-H and C=C Bonds by a Mononuclear Nonheme High-Spin Iron(III)−Alkylperoxo Species

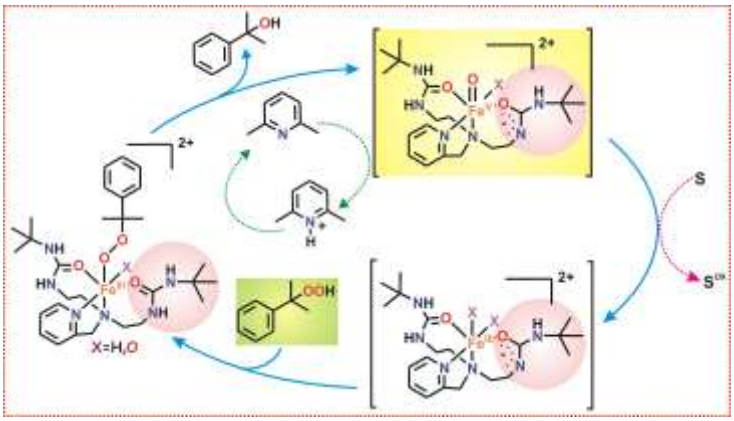

Urea Group is the Player: A transient ($t_{1/2}$ = 3 min at 283 K) high-spin iron(III)-alkylperoxo intermediate supported by a ligand bearing urea groups exhibits selective and catalytic OAT and HAT reactions in the presence of a general base promoter. The urea groups on the ligand backbone plays pivotal role in driving the selectivity and catalytic activity.